


[View Journal Online](#)
[View Article Online](#)

Molecular dynamics of fibric acids

Chad Miller , Steven Schildcrout , Howard Mettee , and Ganesaratnam Balendiran *

Department of Chemistry, Youngstown State University, Youngstown, OH 44555, U.S.A.

* Corresponding author at: Department of Chemistry, Youngstown State University, Youngstown, OH 44555, U.S.A.
e-mail: gkbalendiran@ysu.edu (G. Balendiran).

RESEARCH ARTICLE

ABSTRACT



doi 10.5155/eurjchem.13.2.186-195.2275

Received: 17 March 2022

Received in revised form: 16 April 2022

Accepted: 22 April 2022

Published online: 30 June 2022

Printed: 30 June 2022

KEYWORDS

Computation
Thermochemistry
Molecular Scaffold
Molecular dynamics
Molecular modeling
Conformational analysis

¹H- and ¹³C-NMR chemical shifts were measured for four fibric acids (bezafibrate, clofibrate, fenofibrate, and gemfibrozil), which are lipid-lowering drugs. Correlation is found with DFT-computed chemical shifts from the conformational analysis. Equilibrium populations of optimized conformers at 298 K are very different when based on computed Gibbs energies rather than on potential energies. This is due to the significant entropic advantages of extended rather than bent conformational shapes. Abundant conformers with intramolecular hydrogen bonding via five-member rings are computed for three fibric acids, but not gemfibrozil, which lacks suitable connectivity of carboxyl and phenoxy groups. Trends in computed atom-positional deviations, molecular volumes, surface areas, and dipole moments among the fibric acids and their constituent conformations indicate that bezafibrate has the greatest hydrophilicity and fenofibrate has the greatest flexibility. Theoretical and experimental comparison of chemical shifts of standards with sufficient overlap of fragments containing common atoms, groups, and connectivity may provide a reliable minimal set to benchmark and generate leads.

Cite this: *Eur. J. Chem.* 2022, 13(2), 186-195Journal website: www.eurjchem.com

1. Introduction

Computational studies are recognized as a useful tool in molecular design and discoveries [1]. Considering the number of software programs, [2] speed of computation, cost of performing computations, and accessibility, the number of compounds that can be theoretically explored is essentially unlimited. Generating a large collection of molecules experimentally would be not only costly but also environmentally damaging. The time to synthesize, purify, and characterize every predicted derivative even in a given class of compounds would be excessive. On the other hand, if theoretical predictions can be validated by experimental methods for a few compounds they can be treated as benchmarked standards against the library of designed compounds to eliminate a large fraction of them and focus only on a few scaffolds. If some specific property of a molecule is found to preclude its intended use, this may permit early-stage elimination of a subclass with this property from further consideration.

To introduce this concept, we present here a computational study of a class of compounds of interest as agents for anti-hypercholesterolemia and diabetes treatment, the four fibric acid derivatives: 2-(4-{2-[(4-chlorobenzoyl)amino]ethyl}phenoxy)-2-methylpropanoic acid (C₁₉H₂₀NO₄Cl), 2-(4-chlorophenoxy)-2-methylpropanoic acid (C₁₀H₁₁O₃Cl), 2-[4-(4-chlorobenzoyl)phenoxy]-2-methylpropanoic acid (C₁₇H₁₅O₄Cl) and 5-(2,5-dimethylphenoxy)-2,2-dimethylpentanoic acid (C₁₅H₂₂O₃),

known respectively as bezafibrate (Beza), clofibrate (Clo), fenofibrate (Fen) and gemfibrozil (Gem) (Figure 1). These fibric acids interact with the diabetes target, aldose reductase, and other members of the aldo-keto reductase family of proteins, AKR1B10 [3-8], and regulate their catalytic activity. In this study, the significant conformations of these four fibric acids are scrutinized, and their predicted and experimental NMR spectra along with other computed molecular properties, are obtained and compared.

2. Experimental

2.1. Molecular computations

The fibric acid structures were initially built using Spartan [9,10], with which a conformer distribution was determined at the semiempirical PM3 level. The resulting conformers were sorted based on potential energies *E*, and the lower-energy conformers within the default limit of 40 kJ/mol were retained. Previously obtained crystal structures of each compound [11-14] were considered also. Conformers were then optimized by density functional theory (DFT) using Gaussian16 [15] through the Ohio Supercomputer Center [16] at the B3LYP/6-31G* level with acetone solvent (as for the NMR experiments) by the self-consistent reaction field (SCRF) method with the polarizable continuum model (PCM) and vibrational analysis (FREQ) to obtain standard thermochemical parameters at 298 K and to

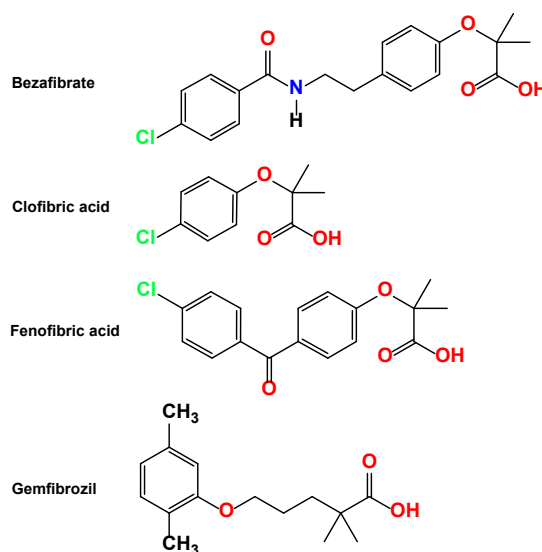


Figure 1. Chemical structures of fibric acids Beza, Clo, Fen, and Gem.

verify that true local minima were obtained with no imaginary frequencies. Boltzmann factors were calculated from Equation (1);

$$\frac{N}{N_a} = \exp\left(-\frac{\Delta G^\circ}{RT}\right) \quad (1)$$

where $\Delta G^\circ = G^\circ - G^\circ_a$. Here G° is the computed standard Gibbs energy for a conformer, and G°_a is for the most stable conformer. Only conformers with Boltzmann factor > 1% are considered significant here. This corresponds to a limit $\Delta G^\circ < 12$ kJ/mol and results in 5, 4, 8, and 7 retained conformers, respectively, for Beza, Clo, Fen, and Gem. Differences in computed entropy (S°) among conformers of each compound, except for Gem, yield significant differences in computed populations and stability rankings based on G° versus E , showing the importance of using G° .

As a test of the basis-set adequacy, the principal conformer of Clo was optimized with B3LYP/6-311+G** giving a geometry close to that with 6-31G*. Torsion angles are within 2° and bond lengths within 0.005 Å between the two basis sets, so the more economical B3LYP/6-31G* method is used for geometry optimizations.

For each of the 24 conformers, NMR spectra were computed using the Gaussian default gauge-independent atomic orbital method with B3LYP/6-311+G**. Chemical shifts were obtained (Equation 2) by subtracting the fibric acid chemical shieldings from those of optimized tetramethylsilane: $\sigma(^1\text{H}) = 31.89$ ppm, $\sigma(^{13}\text{C}) = 184.0$ ppm.

$$\delta_{\text{calc}} = \sigma_{\text{ref}} - \sigma \quad (2)$$

The carboxylic acid and amide protons are not considered in this analysis because their σ depends on experimental temperature and concentration, and cannot be reliably compared with the theoretical calculations [17,18]. For comparison with experimental values, predicted chemical shifts are averaged for atoms that are expected to experience the same electronic environment within the NMR timescales (e.g., protons in the same methyl group).

To create composite NMR spectra from the ensembles of predicted spectra, the chemical shifts are weighted according to the Boltzmann factors of the conformers. Since the structural computations show the most abundant conformers with intramolecular H bonding for Beza (**a** and **b**), Clo (**a** only), and

Fen (**a** and **b**), weighted averages of the computed NMR spectra for these conformers are used for comparison with experiment. For Gem, with no evident H bonding, the **a** and **b** conformers are used.

Preliminary computations suggest possible intermolecular hydrogen-bonding between an individual acetone molecule through its O atom and a proton at a carboxyl or amide site of the fibric acid. These are not considered in the modeled geometries and NMR spectra reported here, although the PCM method does recognize the electrical environment of the solvent. Comparison of the modeled and the observed NMR spectra may indicate the extent of such specific solvation.

Van der Waals (vdW) volume is calculated using the vdW radius of every atom at its position and includes all atoms in the molecule. The surface enclosing the vdW volume is the vdW surface [19-21]. The solvent-accessible surface is defined as the exterior area surrounded by the solvent probe (radius 1.4 Å) around the molecule. This probe radius reflects the role of the O atom since the acetone solvent is a polar, hydrogen bond acceptor only. Calculation of polar surface area (PSA) has been described [22,23].

2.2. NMR measurements of fibric acids

The spectra were recorded at 300 K on a Bruker Avance III 400 MHz NMR with a broadband probe and analyzed using the Bruker Topspin software package [24]. Bezafibrate (Sigma lot: 046k1113), gemfibrozil (Sigma lot: 65H0084), and clofibrac acid (Aldrich lot: 01220BT) were purchased commercially and used without further modification. Fen was synthesized from fenofibrac as previously reported and characterized [12]. Each compound was dissolved in acetone- d_6 (99.9 atom % D) with 0.3% TMS, purchased from Sigma. ^1H spectra utilized the zg30 pulse program [24], with digital quad detection (DQD) acquisition mode. For each spectrum, 128 scans were collected with a D1 delay of 2.0 s; a 90° pulse time of 7.83 μs; a sweep width (sw) range of 20.55-20.68 ppm; o1 signal range of 2470.79-2471.09 Hz; and the receiver gain set to 143.7 for Beza, 645.1 for Clo, 12.7 for Gem, and 181 for Fen. ^{13}C spectra were run proton decoupled (pulse program zpgp30) with qsim acquisition mode, 1024 scans, a 90° pulse time of 14.90 μs, and a D1 delay of 2.0 s. The sw range was 238.32-238.88 ppm, the ^{13}C o1 range was 10060.80-10061.31 Hz, the ^1H o2 range was 1600.52-1600.60 Hz, and the receiver gain was 181 for Beza, 203.2 for Clo, and 2050 for Fen and Gem.

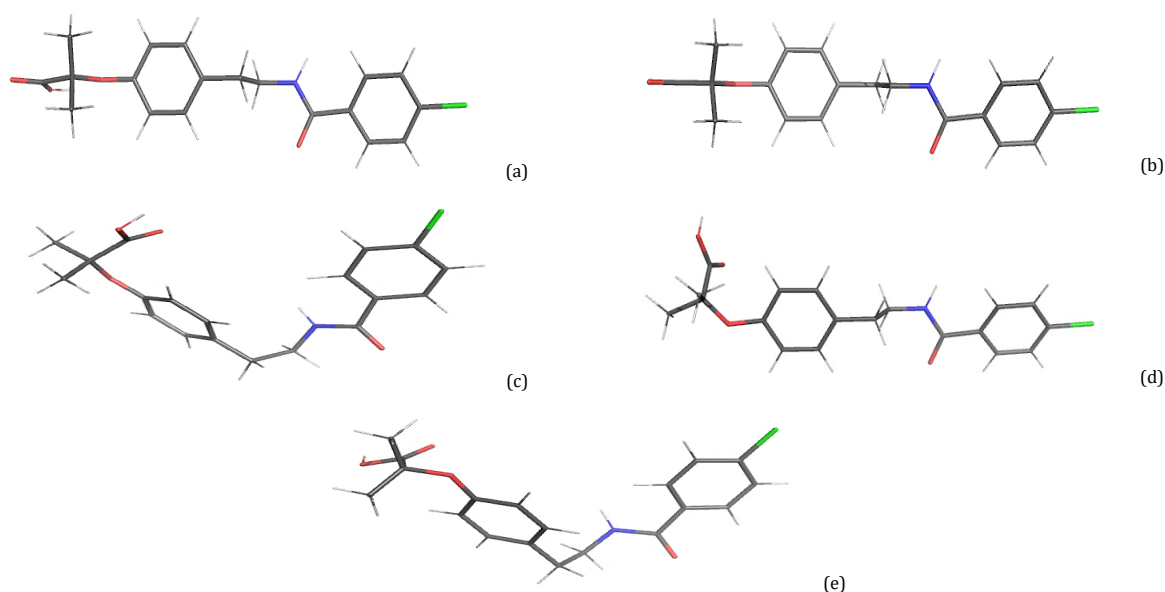
Table 1. Absolute thermochemical parameters of fibric acid conformers in acetone solvent from optimized geometries by B3LYP/6-31G(d) polarizable continuum model. Conformers are ordered by increasing G_{298}° . 1 a.u. (atomic unit) = 1 hartree = 2625.5 kJ/mol

Fibric acid	Conformer	E (a.u.)	H_{298}° (a.u.)	S_{298}° (J/mol K)	G_{298}° (a.u.)
Beza	a	-1551.958624	-1551.573556	751.24	-1551.658867
	b	-1551.958985	-1551.573846	740.48	-1551.657934
	c	-1551.956908	-1551.571759	747.05	-1551.656595
	d	-1551.956749	-1551.571648	739.40	-1551.655610
	e	-1551.956865	-1551.571683	733.87	-1551.655022
Clo	a	-1073.570292	-1073.361509	519.19	-1073.420470
	b	-1073.568426	-1073.359748	504.34	-1073.417021
	c	-1073.570038	-1073.361119	488.11	-1073.416547
	d	-1073.569192	-1073.360291	491.91	-1073.416150
Fen	a	-1417.958000	-1417.651744	653.58	-1417.725963
	b	-1417.958077	-1417.651803	648.90	-1417.725489
	c	-1417.959693	-1417.653271	631.74	-1417.725009
	d	-1417.959552	-1417.653115	632.62	-1417.724954
	e	-1417.959651	-1417.653206	631.62	-1417.724933
	f	-1417.959585	-1417.653195	631.32	-1417.724889
	g	-1417.958871	-1417.652434	635.13	-1417.724560
	h	-1417.958749	-1417.652313	635.47	-1417.724477
Gem	a	-810.554084	-810.187362	635.21	-810.259495
	b	-810.551948	-810.185132	635.38	-810.257284
	c	-810.551900	-810.185072	633.37	-810.256998
	d	-810.551070	-810.184255	634.75	-810.256338
	e	-810.550508	-810.183680	635.38	-810.255835
	f	-810.550398	-810.183528	634.80	-810.255614
	g	-810.550324	-810.181802	634.88	-810.255567

Table 2. Beza conformers in acetone, ΔG° and Boltzmann factor for 298 K with dipole moments by B3LYP/6-31G*, solvent-accessible volumes and total and polar surface areas, and atom-positional RMSDs**.

Conformer / 45 atoms	ΔG° (kJ/mol)	Boltzmann factor	μ (D)	Volume (\AA^3)	Surface (\AA^2)	PSA (\AA^2)	RMSD (\AA)
a	0.00	1.000	6.80	371	352	61.3	0
b	2.45	0.372	6.65	373	352	61.4	1.12
c	5.97	0.090	5.89	376	351	63.2	3.44
d	8.55	0.032	7.17	370	356	63.8	1.48
e	10.10	0.017	7.38	381	349	63.2	2.95

** Weighted average RMSD = 0.546 \AA .

**Figure 2.** Five B3LYP/6-31G* optimized bezafibrate conformers.

3. Results

Fibric acids are a class of molecules with various molecular architectures though some contain halogen, oxy, dimethyl, and aromatic group(s) as common functionalities. They differ in size, number and type of atoms, bonds, connectivity, and functional groups in addition to substitutions between oxy and dimethyl groups.

3.1. Fibric acid conformers

The significant conformers of Beza, Fen, Clo, and Gem are shown in Figures 2-5. A table of optimized E and H° , S° , and G° at 298 K for each conformer is in Table 1. Their relative free energies, N/N_a Boltzmann populations, vdW solvent-accessible surface area, volume, dipole moments, and RMSD relative to the most stable conformation are shown in Tables 2-5. VdW volume and surface areas, which are independent of conformer for each acid, are shown in Table 6.

Table 3. Clo conformers in acetone, ΔG° and Boltzmann factor for 298 K with dipole moments by B3LYP/6-31G*, solvent-accessible volumes and total and polar surface areas, and atom-positional RMSDs**.

Conformer / 25 atoms	ΔG° (kJ/mol)	Boltzmann factor	μ (D)	Volume (\AA^3)	Surface (\AA^2)	PSA (\AA^2)	RMSD (\AA)
a	0.00	1.000	3.32	211	207	37.3	0
b	9.06	0.026	2.57	212	208	40.1	1.50
c	10.30	0.016	3.05	210	210	39.9	2.15
d	11.34	0.010	5.04	210	210	39.7	2.10

** Weighted average RMSD = 0.090 \AA **Table 4.** Fen conformers in acetone, ΔG° and Boltzmann factor for 298 K with dipole moments by B3LYP/6-31G*, solvent-accessible volumes and total and polar surface areas, and atom-positional RMSDs**.

Conformer / 37 atoms	ΔG° (kJ/mol)	Boltzmann factor	μ (D)	Volume (\AA^3)	Surface (\AA^2)	PSA (\AA^2)	RMSD (\AA)
a	0.00	1.000	2.88	314	299	51.5	0
b	1.24	0.605	3.10	317	299	51.5	2.07
c	2.50	0.364	4.88	315	303	54.0	2.24
d	2.65	0.343	4.97	314	302	54.0	2.14
e	2.70	0.336	4.98	316	304	54.0	2.06
f	2.82	0.321	5.07	314	302	54.0	1.96
g	3.68	0.226	7.00	316	303	53.8	1.37
h	3.90	0.207	6.32	313	302	53.8	2.10

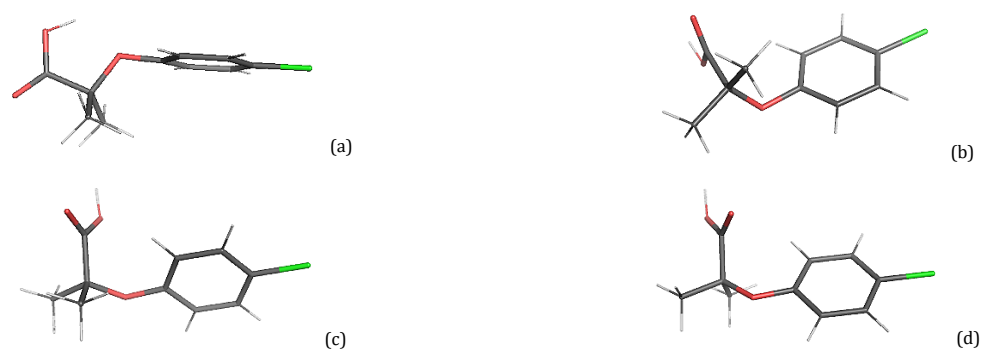
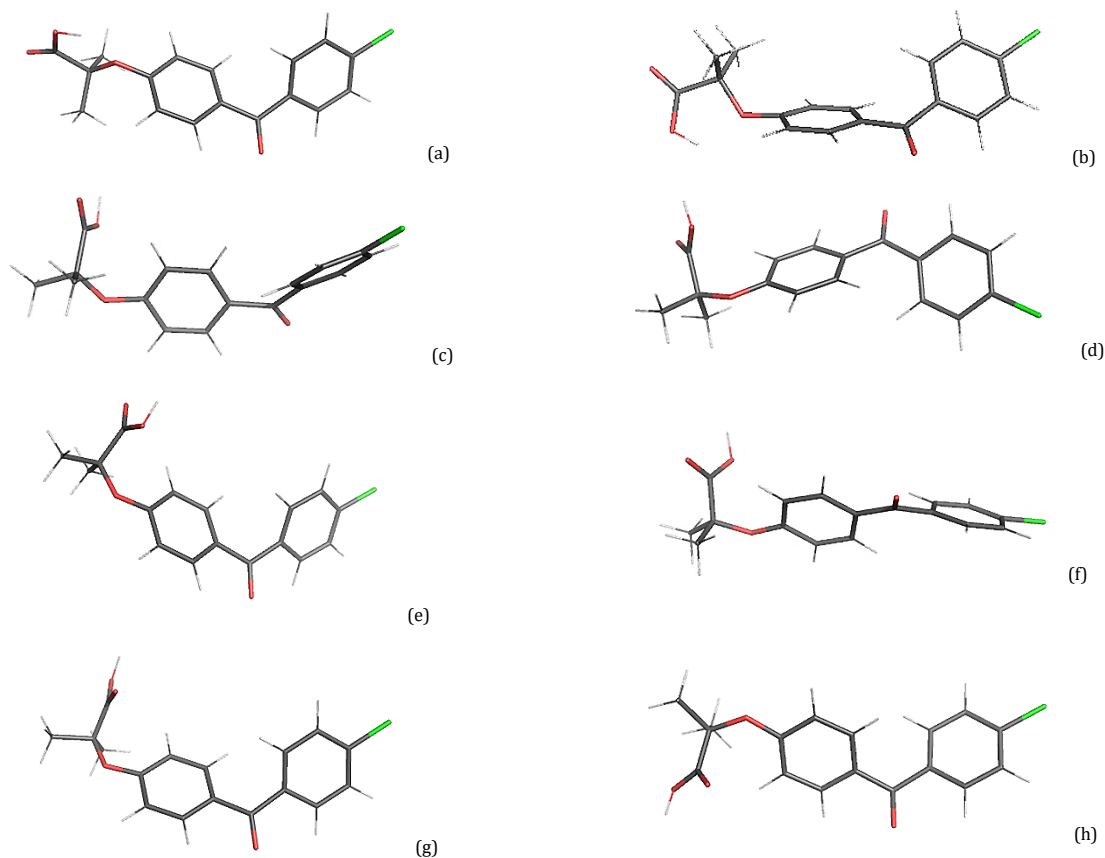
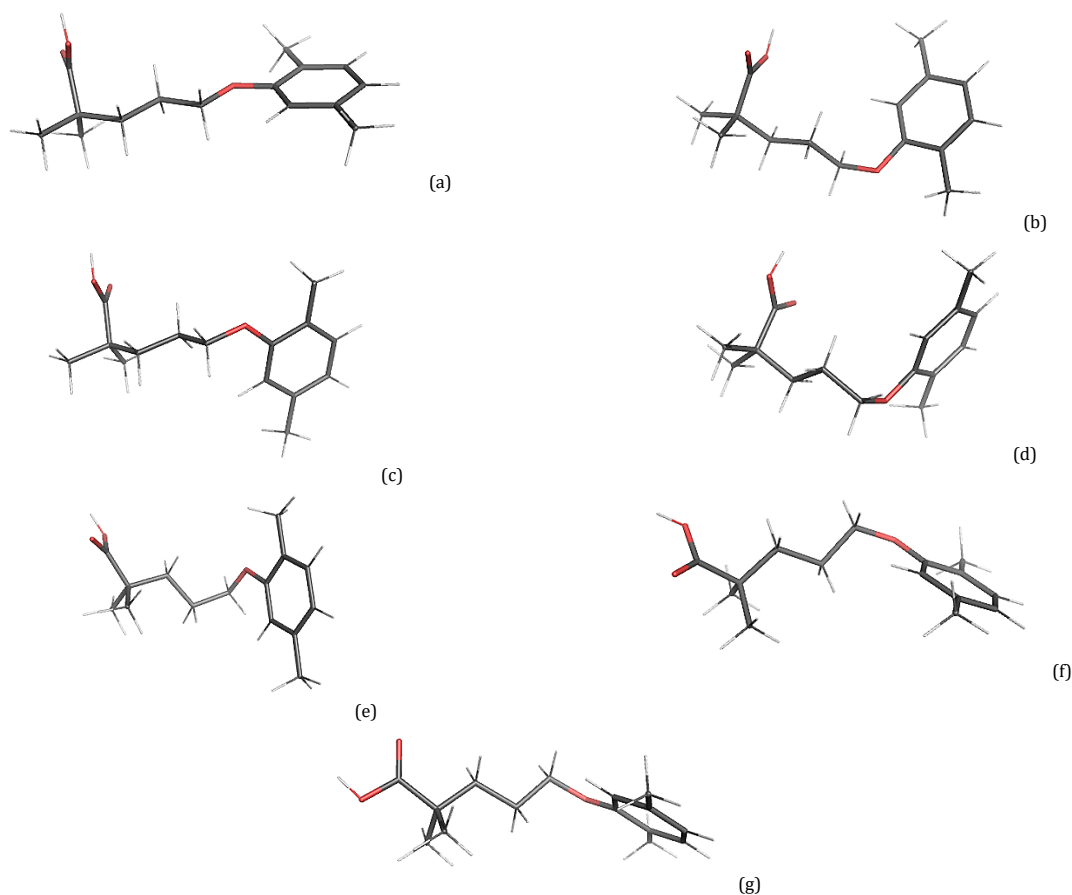
** Weighted average RMSD = 1.430 \AA **Figure 3.** Four B3LYP/6-31G* optimized clofibric acid conformers.**Figure 4.** Eight B3LYP/6-31G* optimized fenofibric acid conformers.

Table 5. Gem conformers in acetone, ΔG° and Boltzmann factors for 298 K with dipole moments by B3LYP/6-31G*, solvent-accessible volumes and total and polar surface areas, and atom-positional RMSDs**.

Conformer / 40 atoms	ΔG° (kJ/mol)	Boltzmann factor	μ (D)	Volume (\AA^3)	Surface (\AA^2)	PSA (\AA^2)	RMSD (\AA)
a	0.00	1.000	3.31	297	287	39.3	0
b	5.80	0.096	3.12	291	286	39.4	2.42
c	6.56	0.071	3.09	293	284	39.4	1.72
d	8.29	0.035	3.60	299	282	39.3	2.10
e	9.61	0.021	3.31	302	281	39.2	2.01
f	10.19	0.016	1.52	291	285	39.3	1.89
g	10.31	0.016	2.50	291	285	39.3	1.90

** Weighted average RMSD = 0.423 \AA .**Table 6.** Van der Waals volumes and surface areas for fibric acids.

Acid	Volume (\AA^3)	Surface (\AA^2)
Beza	332	385
Clo	191	228
Fen	285	326
Gem	261	309

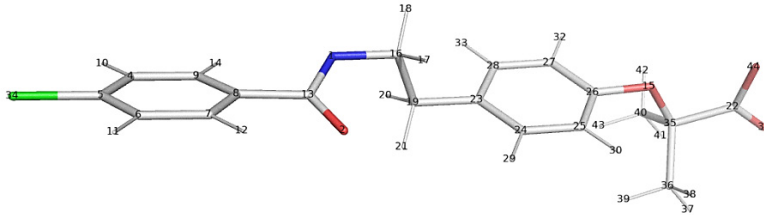
**Figure 5.** Seven B3LYP/6-31G* optimized gemfibrozil conformers.

Polar surface areas (PSA) are shown for all significant conformers of each fibric acid in Tables 2-5. PSAs are used to estimate molecular transport through membranes and consider the surface area of the electronegative N and O atoms with any attached H atoms. Such sites are likely to involve hydrogen bonding. Lower PSA is associated with more facile permeation of barriers [22,23]. In the present calculations, conformers with an intramolecular hydrogen bond show small but significant decreases in PSA, 2 to 3 \AA^2 , compared to the others. The ranking among the fibric acids is Beza > Fen > Gem \approx Clo, reflecting the counts of N and O atoms per molecule, respectively, 5, 4, 3, and 3.

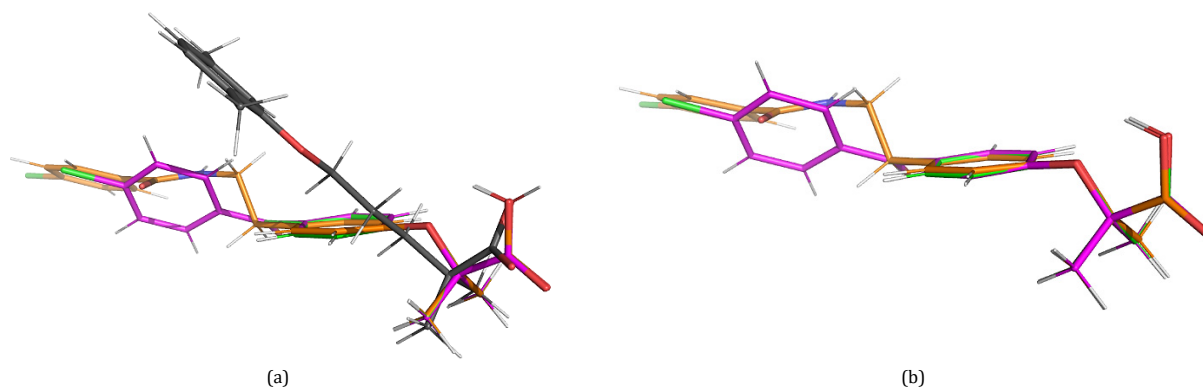
Similarities between two conformations or fragments are reported as atom-positional RMSDs by determining the difference (deviation) in the coordinates of atoms that are of the identical type and the same connectivity. Comparison (Figure 6) of the 13-atom fragment 2-methylpropanoic acid,

Me_2CCOOH , common to all four fibric acids, also reveals very similar fragment conformations among these molecules versus that of Clo, except for Gem, with RMSD values 0.009, 0.036, and 0.641 \AA for Fen, Beza, and Gem, respectively (Figure 6a). The larger RMSD for Gem reflects the *syn* conformation of its carboxyl group, while in the other three acids, the carboxyl is *anti* to accommodate the intramolecular hydrogen bond to the ether function. The absence of this bond and a close phenoxy group in Gem due to a fragment with a different connectivity results in its variant conformation.

The 24-atom fragment, phenoxy-2-methylpropanoic acid, $\text{PhOCMe}_2\text{COOH}$, contained in the lowest- G° conformers of Beza versus Clo and Fen versus Clo have RMSD of 0.117 and 0.015 \AA , respectively (Figure 6b). These low values suggest that this fragment in Clo, Fen, and Beza has very similar lowest-energy conformations in each compound, but this fragment is absent in Gem.

Table 7. Theoretical (B3LYP/6-311+G**) and experimental ^1H and ^{13}C NMR chemical shifts for bezafibrate in acetone.


Hydrogen(s) (atom number)	$\delta_{\text{theor.}}$ (ppm)	$\delta_{\text{exp.}}$ (ppm)
Methyl (37-39, 41-43)	1.48	1.55
CH ₂ , adj. to phenyl (20-21)	2.91	2.85
CH ₂ , adj. to amide (17-18)	3.47	3.58
Phenyl (30, 32)	7.40	6.84
Phenyl (29, 33)	7.65	7.16
Phenyl (10-11)	7.70	7.50
Phenyl (12, 14)	8.03	7.87
Carbon(s) (atom number)	$\delta_{\text{theor.}}$ (ppm)	$\delta_{\text{exp.}}$ (ppm)
Methyl (36, 40)	26.0	26.6
CH ₂ adj. to phenyl (19)	41.6	35.5
CH ₂ adj. to amide (16)	48.8	42.3
Quaternary (35)	91.3	79.5
Phenyl (25, 27)	138.2	120.1
Phenyl (4, 6)	135.7	129.3
Phenyl (7, 9)	135.7	129.8
Phenyl (24, 28)	137.4	130.3
Phenyl adj. to amide (8)	141.2	134.0
Phenyl adj. to CH ₂ (23)	146.4	134.8
Phenyl adj. to Cl (5)	153.9	138.7
Phenyl adj. to O (26)	159.4	155.0
Amide (13)	173.9	166.2
Carboxyl (22)	185.9	175.6

**Figure 6.** (a) Atom by atom superposition of fibric acids based on 13-atom fragments that are identical and maintain the same connectivity. (b) Atom by atom superposition of fibric acids based on 24-atom fragments that are identical and maintain same connectivity. Since Gem lacks the phenoxy fragment connectivity it is not included in the 24-atom overlay. Molecular color: Beza - beige, Fen - pink, Clo - green, Gem - gray. Atom color: Cl - green, O - red, N - blue, C - color of fibric acid, H - white. All fibric acids are compared against the smallest member, Clo.

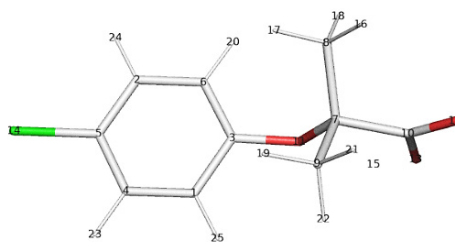
Clo has all most common functional groups found in the class of fibric acids. Fen has an additional aromatic ring, but it is part of a benzophenonyl group, and it differs from Beza by the number of atoms and groups linking the two aromatic rings. Gem has only one aromatic ring but a linker with three adjacent methylene groups, the most out of the fibric acids, whereas Beza has only two. The computations show each of the fibric acids with one or two of its most abundant conformers containing an intramolecular hydrogen bond between the carboxyl and the ether groups, except for Gem, where these groups are farther apart. These bonds are found in Beza **a** and **b**, Clo **a**, and Fen **a** and **b**. Each such bond gives a near-planar five-member ring with an O...H distance of 1.84 Å, which accounts for the *anti*-conformation of the carboxyl group rather than the usually preferred *syn* [25] as found for other conformers.

For Clo, the **a** conformer has 95% of the Boltzmann population and is the only one with a plane of symmetry. Besides having the most favorable G° , **a** also has the most favorable E and S° . The other three conformers **b-d**, with no H

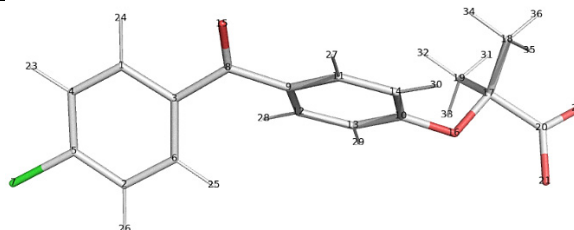
bonding and *syn* carboxyl groups, have G° 9 to 12 kJ/mol less negative, giving similar low populations.

Beza's conformers **a** and **b** account for over 90% of the computed Boltzmann population. They have G° within 2.5 kJ/mol of each other and are the only two Beza conformers with elongated, rather than bent, shapes and an intramolecular hydrogen bond between the carboxyl H atom and the ether O atom. The two differ in the signs of approximately $\pm 90^\circ$ respective torsion angles about the N1-C16 bond (N to methylene C) and the C19-C23 bond (the other methylene C to an aromatic C). Optimization of the observed crystal structure [11] gives the **d** conformer.

Only Beza among these fibric acids has an amide group. The amide N-C bond length is near 1.36 Å, consistent with significant double-bond character [26] and limited torsion. This is supported by the computed NMR results, which show the two phenyl atoms C7 and C9 to be non-equivalent, with the C *cis* to the amide O more deshielded by δ 4.4 ppm compared to the C *cis* to the N. The average δ for these two C atoms is in Table 6.

Table 8. Theoretical (B3LYP/6-311+G**) and experimental ¹H and ¹³C NMR chemical shifts for clofibric acid in acetone.

Hydrogen(s) (atom number)	$\delta_{\text{theor.}}$ (ppm)	$\delta_{\text{exp.}}$ (ppm)
Methyl (16-19, 21-22)	1.48	1.59
Phenyl (20, 25)	7.36	6.94
Phenyl (23-24)	7.62	7.3
Carbon(s) (atom number)	$\delta_{\text{theor.}}$ (ppm)	$\delta_{\text{exp.}}$ (ppm)
Methyl (8, 9)	25.9	25.5
Quaternary (7)	92.0	80.0
Phenyl (1, 6)	134.5	121.6
Phenyl (2, 4)	136.4	127.3
Phenyl adj. to Cl (5)	147.0	129.9
Phenyl adj. to O (3)	159.9	155.5
Carboxyl (10)	185.5	175.1

Table 9. Theoretical (B3LYP/6-311+G**) and experimental ¹H and ¹³C NMR chemical shifts for fenofibric acid in acetone.

Hydrogen(s) (atom number)	$\delta_{\text{theor.}}$ (ppm)	$\delta_{\text{exp.}}$ (ppm)
Methyl (31-36)	1.54	1.68
Phenyl (29-30)	7.54	7.00
Phenyl (23, 26)	7.79	7.57
Phenyl (24-25)	8.24	7.76
Phenyl (27-28)	8.18	7.77
Carbon(s) (atom number)	$\delta_{\text{theor.}}$ (ppm)	$\delta_{\text{exp.}}$ (ppm)
Methyl (18-19)	26.2	25.7
Quaternary (17)	92.9	80.0
Phenyl (13-14)	132.7	118.4
Phenyl (2, 4)	135.5	129.4
Phenyl bonded to ketone (9)	142.4	131.2
Phenyl (1, 6)	140.0	132.0
Phenyl (11-12)	140.0	132.6
Phenyl bonded to ketone (3)	143.5	137.8
Phenyl bonded to Cl (5)	156.1	138.4
Phenyl bonded to O (10)	166.1	160.8
Carboxyl (20)	185.3	174.8
Ketone (8)	204.1	194.0

All conformers show the amide group as the *trans* isomer, which is understandable since a hypothetical *cis* form would force a close approach, less than 2 Å, between a proximal-methylene H atom and a chlorophenyl H at an energy cost of over 30 kJ/mol.

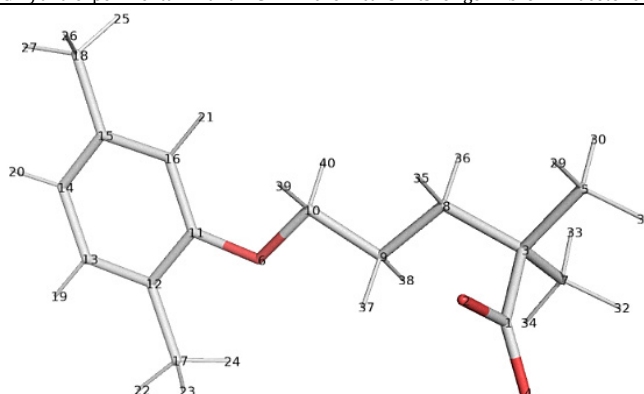
The O atom of the amide linker in Beza may seem to provide an option to form an intramolecular hydrogen bond with the carboxyl H. Although two such conformers with bent shapes were found, they have negligible populations due to S° about 60 J/mol.K less than those of the conformers **a-e** considered here without this bond. This decreased S° makes G° less negative by nearly 20 kJ/mol.

Beza, with longer flexible linkers and more hindered rotations than Clo, conquers more theoretically observed conformers. Among them, the presence of CH₂ groups tends to achieve more highly stable conformers than Clo, with no methylene moieties. In addition, Beza shows greater variations within its low- G° conformers.

Fen is characterized by its chlorobenzophenone group bonded to the ether O. The main geometric difference between

the two most populous and H-bonded conformers **a** and **b** is the sign of the approximately $\pm 90^\circ$ respective torsion angles about the bond between the ether O and the aromatic ring. The more favorable G° of **a** and **b** are due to their high S° rather than their E , which are less favorable than those of **c-h**. Fen has the largest number of conformers with $\Delta G^\circ < 4$ kJ/mol, which are thermochemically accessible with large Boltzmann factors.

Gem, like Beza, has a long flexible linker and several conformers with significant populations. Without intramolecular hydrogen bonding, each of the Gem conformers shows a *syn* carboxyl group. The dominant conformer **a** results from optimizing the reported crystal structure [13]. All its skeletal atoms are coplanar except for the carboxyl group and one of its opposed methyl C atoms, which are in another, perpendicular plane. For the seven conformers, the ordering by G° is the same as the ordering by E since each has essentially the same $S^\circ = 634 \pm 1$ J/mol.K. This is the narrowest conformer-entropy range of all the fibric acids.

Table 10. Theoretical (B3LYP/6-311+G**) and experimental ^1H and ^{13}C NMR chemical shifts for gemfibrozil in acetone.

Hydrogen(s) (atom number)	$\delta_{\text{theor.}}$ (ppm)	$\delta_{\text{exp.}}$ (ppm)
Methyl (29-34)	1.28	1.22
CH ₂ (35-38)	1.74	1.74
Methyl (22-24)	2.24	2.91
Methyl (25-27)	2.38	2.97
CH ₂ (39, 40)	3.86	3.88
Phenyl (21)	6.80	6.64
Phenyl (20)	6.86	6.60
Phenyl (19)	7.26	6.94
Carbon(s) (atom number)	$\delta_{\text{theor.}}$ (ppm)	$\delta_{\text{exp.}}$ (ppm)
Phenyl methyl (17)	19.7	16.2
Phenyl methyl (18)	23.4	21.7
CH ₂ (9)	30.8	25.6
Methyl (5, 7)	40.2	26.1
CH ₂ (8)	41.3	37.8
Quaternary (3)	50.0	42.5
CH ₂ (10)	72.2	68.7
Phenyl (16)	115.0	114.8
Phenyl (14)	126.1	121.6
Phenyl (12)	131.9	124.0
Phenyl (13)	136.4	131.1
Phenyl (15)	146.4	137.1
Phenyl (11)	166.2	158.0
Carboxyl (1)	189.8	181.0

Intramolecular interactions play a significant role in some conformations in fibric acids. Compared to the three other conformers of Clo, only **a** has the suitable angle and the distance of 1.837 Å between the COOH proton and ether O to form an intramolecular hydrogen bond with a nearly planar five-member ring. The situation is similar with the intramolecular hydrogen bonds seen in the extended conformations **a** and **b** for Beza and Fen, but not for Gem where the spacer atoms separate the relevant H and O.

3.2. Theoretical and experimental NMR spectral correlation

The chemical shift values obtained by experimental ^1H and ^{13}C NMR spectra of Beza, Clo, Fen and Gem in acetone-*d*₆ are shown in Tables 7-10 along with those predicted by theory. Atom numbers correspond to the molecular diagram below each table.

Chemical shifts of groups that are part of the 24-atom fragment show varying consistency. ^1H NMR of methyl groups revealed similar theoretical and experimental values in all four fibric acid standards. Among these standards, the ^1H NMR chemical shift of methyl groups is the lowest and deviates from that in the rest of the standards in both theoretical and experimental values though this group will be preserved in the 13-atom fragment in all. Aromatic proton chemical shifts of standards where the 24-atom fragment exists are coherent among them and between theoretical and experimental values.

Not only are the theoretical values of the carboxyl ^{13}C chemical shifts the same in all standards, the correlation with experimental values is consistent as well, but the corresponding values for Gem are at higher fields.

The most striking observation is found in the quaternary ^{13}C of the standard in the fragment that is a signature of fibric acids. The experimental chemical shift is preserved in Beza, Clo, and Fen, and the correlation with theoretical value in these standards is sustained too. However, the chemical shift of this nucleus in the conserved fragment deviates by about 40ppm.

Dimethyl ^{13}C chemical shifts of fragments of fibric acid standards are reliably predictable in all standards except Gem (atom 5, 7), in which the theoretical varies significantly. The 13-atom fragment including this group is preserved in all the standards, but significant change is reflected in the chemical shift and the RMSD among them.

The 4-chloropheno fragment is common to Beza, Clo, and Fen but connectivity is different in the rest of the molecule. The ^{13}C chemical shift fluctuate noticeably among them and the deviation between the theoretical and experimental are different too. However, the ^{13}C shifts of the atom bonded to Cl show similar trends and differences in Beza and Fen though this fragment is connected to the carbonyl group of an amide or ketone. Whereas the ^{13}C atom bonded to the O of the phenoxy fragment, regardless of the aromatic substitution and the fragment connected, it seems to maintain the chemical shift and the difference between the theoretical and experimental values consistently in all standards.

Utilizing three standards with the 24-atom fragment highlights the validity of the theoretical and experimental correlation whereas including the 13-atom fragment with less common atomic composition and connectivity brings out the differences due to connectivity.

4. Discussion

All fibric acids have in common the core fragments phenoxy and 2-dimethylpropanoic acid with similar chemical connectivities, but there are distinguishing features among them which are considered here.

Comparison among each fibric acid considering its low- G° conformations identified in the computational study reveals their flexibilities. Beyond the flexibility of a single conformer due to its vibrational motion, adjustability of the conformer ensemble can be characterized by an average atom-positional RMSD using all atoms, weighting each conformer's RMSD relative to the **a** conformer according to its Boltzmann population. This gives, in increasing order (Tables 2-5) Clo < Gem < Beza < Fen. Clo has low adaptability because it has few hindered rotations. Also, its conformer **a** is much more stable than the others, which all have low availability and small populations. Fen has high flexibility because it has many low energy (available) conformations with substantial populations.

The Ph-O-C fragment is planar in all conformers except the **a** and **b** of Clo, Beza, and Fen. Thus, rotation about the Ph-O bond seems to contribute only limited flexibility, not as expected for an ether with an sp^3 O atom. The computed geometries show C-O-C angles consistently near 120° for all conformers of the fibric acids, implying nominal ether O atoms with sp^2 character. The unshared electrons on O would tend to conjugate with the π system of the aromatic ring, as in molecular phenol, giving double bond character to the Ph-O bond, whose length in the fibric acids is computed near 1.38 \AA , while the other O-C bond length is near 1.45 \AA as for a saturated ether.

As Tables 1-5 show, variations in vdW and solvent-accessible volumes and surface areas among the conformers of a given compound are slight, but there is consistent ranking among the fibric acids, namely Beza > Fen > Gem > Clo with Fen and Gem relatively close. If these properties simply followed the number of atoms per molecule, one would expect Beza > Gem > Fen > Clo, but the different elemental compositions of especially Gem versus Fen account for the computed ranking. Dipole moments show moderate variation among conformers of the same fibric acid. Beza conformers have significantly greater μ than those of the other three compounds. This is attributed to its larger size and amide group, suggesting a greater hydrophilicity for Beza.

Differences between calculated and experimental NMR chemical shifts are expected to the extent that specific solute-solvent interactions occur [27]. Comparisons of these δ for the fibric acid derivatives imply that the calculated shifts may be used to establish reference sets to predict and monitor during generation of selected drug designs and identify ones that are outliers, which may indicate unusual properties reflected by a structure or an unanticipated outcome. Such results may become valuable if caught in the early stages, allowing either a focusing or redirection of the long-term approach.

Among the four acids, Gem tends to be an exception to the trends shown by the others because of its absence of the oxy function at the quaternary C atom, which precludes an intramolecular hydrogen bond. Experimental and computed NMR results for this sp^3 C atom at the 2-position of the propanoic acid fragment reflect this, with the C atom δ 40 ppm more deshielded for Beza, Clo, and Fen, where it is adjacent to a phenoxy O atom, than for Gem where it is adjacent to a trimethylene chain instead.

To initiate an early elimination step in the design of molecules, the fibric acids selected here will serve as a training set to benchmark the structural correlations between theoretical and experimental investigations of the phenoxy and methyl propanoic acid fragments. Furthermore, the methods and the steps utilized reflect their validity for the use as the

training set. The results and the strategy may become useful in selectively choosing only the more promising scaffolds in order to construct benchmark leads. Since characterization of compounds is a necessary step and the NMR technique has been one of the routine methods in practice to validate the identity of newly generated molecules, the comparison of the predicted and experimental spectra will allow recognition of discrepancies between them.

5. Conclusions

All fibric acids have similarities, but this study reveals their differences despite the common fragments that constitute them. Most importantly, the derivatives containing the same fragments but different connectivities show different Boltzmann populations of conformers and hence different molecular properties, such as whether intramolecular hydrogen bonding may occur. For such flexible molecules, populations need to be computed from Gibbs energies, not optimized potential energies. Correlation between the predicted and experimental NMR chemical shifts tends to deviate significantly when the same fragment has different chemical connectivity as seen as in Gem compared to the other fibric acid standards. Differences in biological activity of the individual fibric acids may not be reflected in that of their individual conformers, since these are expected to interconvert rapidly to maintain their equilibrium populations *in vivo* as well as *in vitro*.

Acknowledgements

We thank Ray Hoff for all the technical assistance with the NMR studies, Dr. Matthias Zeller for helpful suggestions at the initial stages of the study and the Ohio Supercomputer Center for computing services, access to the computing systems, extended support, and use of the facility.

Disclosure statement

Conflict of interest: The authors declare no competing financial interests. Ethical approval: All ethical guidelines have been adhered.

Funding

This work is supported by grants from the National Institute of Diabetes and Digestive and Kidney Diseases of the National Institutes of Health and from the Ohio Supercomputer Center.

CRedit authorship contribution statement

All the authors contributed to Conceptualization, Methodology, Calculation, Validation, Analysis, Investigation, Resources, Data Curation, and Writing of this study.


ORCID and Email


Chad Miller

 cmiller@ysu.student.edu

 <https://orcid.org/0000-0002-2087-6566>

Steven Schildcrout

 smschildcrout@ysu.edu

 <https://orcid.org/0000-0002-7176-1726>

Howard Mettee

 hmettee2@hushmail.com

 <https://orcid.org/0000-0001-8210-8119>

Ganesaratnam Balendiran

 pl_note@yahoo.com

 gkbalendiran@ysu.edu

 <https://orcid.org/0000-0003-4604-1038>

References

- [1]. Gund, P.; Andose, J. D.; Rhodes, J. B.; Smith, G. M. Three-dimensional molecular modeling and drug design. *Science* **1980**, *208*, 1425–1431.
- [2]. Sicho, M.; Liu, X.; Svozil, D.; van Westen, G. J. P. GenUI: interactive and extensible open source software platform for de novo molecular generation and cheminformatics. *J. Cheminform.* **2021**, *13*, 1758–2946.
- [3]. Balendiran, G. K.; Balakrishnan, R. In search of aldose reductase inhibitors; Vol. 12, p 276-283, ISBN 9781557533845. Purdue University Press: West Lafayette, IN, 2004. <http://www.thepress.purdue.edu/titles/format/9781557533845> (accessed April 10, 2022)
- [4]. Balendiran, G. K.; Balakrishnan, R. Fibrates inhibit aldose reductase activity in the forward and reverse reactions. *Biochem. Pharmacol.* **2005**, *70*, 1653–1663.
- [5]. Klemm, S.; Calvo, R. Y.; Bond, S.; Dingess, H.; Rajkumar, B.; Perez, R.; Chow, L.; Balendiran, G. K. WY 14,643 inhibits human aldose reductase activity. *J. Enzyme Inhib. Med. Chem.* **2006**, *21*, 569–573.
- [6]. Balendiran, G.; Verma, M.; Perry, E. Chemistry of fibrates. *Curr. Chem. Biol.* **2007**, *1*, 311–316.
- [7]. Balendiran, G. K.; Verma, M.; Bharadwaj, S. Lead Optimization in the Design of Aldose Reductase Inhibitors; Vol. 13, p 228-237, ISBN 978-1-55753-447-7. Purdue University Press: West Lafayette, IN, 2007. <http://www.thepress.purdue.edu/titles/format/9781557534477> (accessed April 10, 2022)
- [8]. Verma, M.; Martin, H.-J.; Haq, W.; O'Connor, T. R.; Maser, E.; Balendiran, G. K. Inhibiting wild-type and C299S mutant AKR1B10; a homologue of aldose reductase upregulated in cancers. *Eur. J. Pharmacol.* **2008**, *584*, 213–221.
- [9]. Kong, J.; White, C. A.; Krylov, A. I.; Sherrill, D.; Adamson, R. D.; Furlani, T. R.; Lee, M. S.; Lee, A. M.; Gwaltney, S. R.; Adams, T. R.; Ochsenfeld, C.; Gilbert, A. T. B.; Kedziora, G. S.; Rassolov, V. A.; Maurice, D. R.; Nair, N.; Shao, Y.; Besley, N. A.; Maslen, P. E.; Dombroski, J. P.; Daschel, H.; Zhang, W.; Korambath, P. P.; Baker, J.; Byrd, E. F. C.; Van Voorhis, T.; Oumi, M.; Hirata, S.; Hsu, C.-P.; Ishikawa, N.; Florian, J.; Warshel, A.; Johnson, B. G.; Gill, P. M. W.; Head-Gordon, M.; Pople, J. A. Q-Chem 2.0: a high-performance ab initio electronic structure program package. *J. Comput. Chem.* **2000**, *21*, 1532–1548.
- [10]. Spartan'20, version 1.0.0, Wavefunction, Inc., Irvine, CA, 2021. <https://wavefun.com> (accessed April 10, 2022).
- [11]. Djinović, K.; Globokar, M.; Zupet, P. Structure of bezafibrate (2-*p*-[2-(*p*-chlorobenzamide)ethyl]phenoxy-2-methylpropanoic acid). *Acta Crystallogr. C* **1989**, *45*, 772–775.
- [12]. Rath, N. P.; Haq, W.; Balendiran, G. K. Fenofibric acid. *Acta Crystallogr. C* **2005**, *61*, o81-4.
- [13]. Bruni, B.; Coran, S.; Di Vaira, M.; Giannellini, V. 5-(2,5-Dimethylphenoxy)-2,2-dimethylpentanoic acid (gemfibrozil). *Acta Crystallogr. Sect. E Struct. Rep. Online* **2005**, *61*, o1989–o1991.
- [14]. Balendiran, G. K.; Rath, N.; Kotheimer, A.; Miller, C.; Zeller, M.; Rath, N. P. Biomolecular chemistry of isopropyl fibrates. *J. Pharm. Sci.* **2012**, *101*, 1555–1569.
- [15]. Frisch, M. J.; Trucks, G. W.; Schlegel, H. B.; Scuseria, G. E.; Robb, M. A.; Cheeseman, J. R.; Scalmani, G.; Barone, V.; Petersson, G. A.; Nakatsuji, H.; Li, X.; Caricato, M.; Marenich, A. V.; Bloino, J.; Janesko, B. G.; Gomperts, R.; Mennucci, B.; Hratchian, H. P.; Ortiz, J. V.; Izmaylov, A. F.; Sonnenberg, J. L.; Williams-Young, D.; Ding, F.; Lipparini, F.; Egidi, F.; Goings, J.; Peng, B.; Petrone, A.; Henderson, T.; Ranasinghe, D.; Zakrzewski, V. G.; Gao, J.; Rega, N.; Zheng, G.; Liang, W.; Hada, M.; Ehara, M.; Toyota, K.; Fukuda, R.; Hasegawa, J.; Ishida, M.; Nakajima, T.; Honda, Y.; Kitao, O.; Nakai, H.; Vreven, T.; Throssell, K.; Montgomery, J. A. J.; Peralta, J. E.; Ogliaro, F.; Bearpark, M. J.; Heyd, J. J.; Brothers, E. N.; Kudin, K. N.; Staroverov, V. N.; Keith, T. A.; Kobayashi, R.; Normand, J.; Raghavachari, K.; Rendell, A. P.; Burant, J. C.; Iyengar, S. S.; Tomasi, J.; Cossi, M.; Millam, J. M.; Klene, M.; Adamo, C.; Cammi, R.; Ochterski, J. W.; Martin, R. L.; Morokuma, K.; Farkas, O.; Foresman, J. B.; Fox, D. J. Gaussian 16, Revision C.01, Gaussian, Inc.: Wallingford CT, 2019.
- [16]. Ohio Supercomputer Center. 1987. Columbus OH: Ohio Supercomputer Center. <http://osc.edu/ark:/19495/f5s1ph73> (accessed April 10, 2022).
- [17]. Stringfellow, T. C.; C. Farrar, T. NMR chemical shift temperature dependence of isocyanomethane. *Spectrochim. Acta A Mol. Biomol. Spectrosc.* **1997**, *53*, 2425–2433.
- [18]. Wendt, M. A.; Meiler, J.; Weinhold, F.; Farrar, T. C. Solvent and concentration dependence of the hydroxyl chemical shift of methanol. *Mol. Phys.* **1998**, *93*, 145–151.
- [19]. Lee, B.; Richards, F. M. The interpretation of protein structures: Estimation of static accessibility. *J. Mol. Biol.* **1971**, *55*, 379–400.
- [20]. Richards, F. M. Areas, volumes, packing and protein structure. *Annu. Rev. Biophys. Bioeng.* **1977**, *6*, 151–176.
- [21]. Connolly, M. L. Analytical molecular surface calculation. *J. Appl. Crystallogr.* **1983**, *16*, 548–558.
- [22]. Krarup, L. H.; Christensen, I. T.; Hovgaard, L.; Frokjaer, S. Predicting drug absorption from molecular surface properties based on molecular dynamics simulations. *Pharm. Res.* **1998**, *15*, 972–978.
- [23]. Clark, D. E. Rapid calculation of polar molecular surface area and its application to the prediction of transport phenomena. 1. Prediction of intestinal absorption. *J. Pharm. Sci.* **1999**, *88*, 807–814.
- [24]. TopSpin; Bruker Topspin software package, (RRID:SCR_014227), <https://www.bruker.com/products/mr/nmr/nmr-software/software/topspin/overview.html> (accessed April 10, 2022).
- [25]. Lim, V. T.; Bayly, C. I.; Fusti-Molnar, L.; Mobley, D. L. Assessing the conformational equilibrium of carboxylic acid via quantum mechanical and molecular dynamics studies on acetic acid. *J. Chem. Inf. Model.* **2019**, *59*, 1957–1964.
- [26]. Hoff, A.; Rath, N.; Lisko, J.; Zeller, M.; Balendiran, G. K. Signature of Glycylglutamic Acid structure. *Int J Biochem Biophys (Alhambra)* **2021**, *9*, 8–15.
- [27]. Bryant, R. G. NMR relaxation studies of solute-solvent interactions. *Annu. Rev. Phys. Chem.* **1978**, *29*, 167–188.



Copyright © 2022 by Authors. This work is published and licensed by Atlanta Publishing House LLC, Atlanta, GA, USA. The full terms of this license are available at <http://www.eurjchem.com/index.php/eurjchem/pages/view/terms> and incorporate the Creative Commons Attribution-Non Commercial (CC BY NC) (International, v4.0) License (<http://creativecommons.org/licenses/by-nc/4.0>). By accessing the work, you hereby accept the Terms. This is an open access article distributed under the terms and conditions of the CC BY NC License, which permits unrestricted non-commercial use, distribution, and reproduction in any medium, provided the original work is properly cited without any further permission from Atlanta Publishing House LLC (European Journal of Chemistry). No use, distribution or reproduction is permitted which does not comply with these terms. Permissions for commercial use of this work beyond the scope of the License (<http://www.eurjchem.com/index.php/eurjchem/pages/view/terms>) are administered by Atlanta Publishing House LLC (European Journal of Chemistry).